JOURNAL OF MATERIALS SCIENCE 23 (1988) 2294–2304

Effect of refining techniques on stress corrosion cracking behaviour of Inconel X-750

B. MISHRA
Tata Iron and Steel Company, Research and Development, Jamshedpur, India
J. J. MOORE
Department of Chemical and Materials Engineering, University of Auckland, New Zealand

High-strength age-hardenable nickel-base superalloy Inconel X-750, is susceptible to severe intergranular stress corrosion cracking (IGSCC) when used in the triple heat-treated condition. In this research, the slow strain-rate technique has been employed to evaluate the stress corrosion cracking susceptibility of alloy X-750 under simulated nuclear pressurized water reactor (PWR) conditions, using an automated autoclave system at $8 \times 10^6 \text{N m}^{-2}$ pressure and 289° C temperature. The alloys produced via electroslag refining (ESR) or vacuum arc refining (VAR) processing routes containing 0.004% and 0.011% sulphur, respectively, were solution annealed at either 1075 or 1240° C for 2 h and water quenched followed by ageing in the 704 to 871° C temperature range for up to 200 h, followed by air cooling or furnace cooling. The scanning electron microscopy performed on fractured surfaces revealed that Inconel X-750 processed through the ESR route, solution annealed at 1240° C for 2 h and water quenched, aged at 871° C for 200 h and furnace cooled provided the best combination of strength, ductility and resistance to SCC. A less sensitized area adjacent to the grain boundary was responsible for the improvement in properties and the alloy X-750 is recommended for PWR applications in the above conditions of processing and heat treatment.

1. Introduction

Severe intergranular stress corrosion cracking (IGSCC) has been reported in the double-aged nickel-rich superalloy Inconel X-750, when used as a structural component in pressurized and boiling water reactors of a nuclear power plant. Microstructural aspects and mechanical properties of Inconel X-750 have been studied following the single ageing treatment in the 704 to 871° C temperature range for up to 200 h [1].

It has been suggested [2] that a single ageing treatment, after a high-temperature solution anneal, results in improved IGSCC resistance due to improved morphology of secondary carbides and intermetallics Because crack propagation under SCC conditions depends on cleanliness and microstructure, a study was conducted on the effect of second-phase particles (carbides and intermetallics) produced by various heat-treatment regimes and the inherent inclusion and sulphur levels on the resistance of Inconel X-750 to IGSCC.

Sulphur species, in the form of both dissolved sulphate ions in the coolant water as well as in the form of sulphide inclusions in the alloy, can influence the IGSCC. There is sufficient evidence [3, 4] that non-metallic inclusions, specifically sulphides, play an important role in the initiation of localized corrosion in alloys. Eklund [5, 6] has studied the initiation of pitting corrosion in stainless and carbon steels concluding that the sulphides and their composition play a key role. The effect of heat treatment on Inconel X-750 has been studied with respect to microstructural changes and grain-boundary chemistry using electron and Auger microscopy following a sequence of thermal treatments in the carbide precipitation temperature zone of 704 to 871° C. A 2 h quench solution treatment at 1075° C was followed by ageing for up to 200 h in this temperature regime. The microstructural data have been correlated with Charpy impact test results, hardness values and modified Huey corrosion test results (ASTM G 28-72) [1].

In the present work, seven model heat treatments, producing wide variations in properties, were selected for study. Different levels of reducible sulphide species in the alloy have been used to compare the refining techniques of ESR and VAR. The ESR process provides an effective way of desulphurizing the alloy, decreasing the inclusion density and controlling the segregation effects. A simulated PWR condition, i.e. 1150 p.s.i. ($8 \times 10^6 \text{N m}^{-2}$) pressure and 289° C temperature, has been used in an automated auto-clave interfaced with a slow strain-rate tester (SSRT), capable of providing slow strain rates down to $8 \times 10^{-8} \text{sec}^{-1}$. Standard ASTM tensile specimens have been tested in the medium, as well as in air, to determine the stress corrosion cracking index, I_{scc}. Fractured specimens were observed in a scanning electron microscope to determine the failure mechanisms.

2. Experimental procedure

Stress corrosion cracking tests were conducted under

0022–2461/88 $03.00 + .12

TABLE I

Element	Chemical composition	
	VIM + VAR	VIM + ESR
Nickel	72.96	72.57
Carbon	0.05	0.04
Manganese	0.002	0.006
Silicon	0.03	0.04
Phosphorus	LT 0.005	LT 0.005
Sulphur	0.011	0.004
Chromium	15.37	15.51
Titanium	2.52	2.45
Aluminium	0.80	0.78
Iron	6.92	7.10
Niobium	0.90	0.89
Boron	0.0045	0.0042
Copper	0.003	*

slow strain-rate conditions. Image analysis for inclusion studies and scanning electron microscopy (SEM) of the fractured surfaces were performed on the failed alloy specimens produced via VIM + ESR and VIM + VAR (vacuum induction melting + vacuum arc refining) processing routes.

Hot-rolled 15.87 mm × 38 mm bars of Inconel X-750 alloy were produced in one vacuum induction melted (VIM) heat which was divided into two lots. One-half of the heat was subsequently processed through the ESR route while the other half was processed though the VAR route, resulting in the compositions shown in Table I.

Specimens cut from the bars were subjected to various heat-treatment cycles comprising solution treatment at 1075° C for 2 h followed by quenching in water. Specimens were then aged at 704° C for 2 h or 200 h, at 760° C for 100 h and at 871° C and 100 h or 200 h followed by cooling in air. Ageing was also performed in a vacuum of 10^{-6} torr at 871° C for 200 h and furnace cooled. The seventh specimen was used in the as-quenched condition. This ageing temperature range, i.e. 704 to 871° C, was selected because of its coincidence with the nose of the TTT curve for this alloy [7]. The completion of all precipitation processes within a reasonable time is possible at these temperatures and a grain-boundary segregation of trace elements, e.g. sulphur, phosphorus, boron, is possible [1]. A high-temperature solution treatment at 1240° C for 2 h followed by water quenching was also conducted to study the effect of grain-size difference between ESR and VAR processed alloys.

Inclusion studies were conducted on both the VIM + VAR and VIM + ESR processed specimens using an image analyser.

The stress corrosion cracking studies were performed on a slow strain-rate tester (SSRT) interfaced with a 0.25 litre autoclave. A motor speed controller unit was used to pick up continuous load signals from a load-cell connected to the pull-rod and displacement signal from a LVDT gauge attached to the vertical mount. A strip chart recorder plotted the load and displacement data. Fig. 1 shows a schematic diagram of the autoclave assembly.

Deionized water was used as the medium for SCC testing. The pH and dissolved oxygen contents of the superheated water environment were recorded at regular intervals. ASTM standard (G49–79) specimens with 1 in. (2.54 cm) gauge length and 0.252 in. (0.64 cm) gauge diameter were used. The specimens were tested at an initial strain rate of $2.8 \times 10^{-6}\,sec^{-1}$.

An acid mixture of 80 ml HNO_3 + 3 ml HF was used to swab-etch optical metallography specimens for 1.5 min.

3. Experimental results

The heat treatments used in this IGSCC study were selected because they provide a wide variation in microstructural changes and hardness values. This

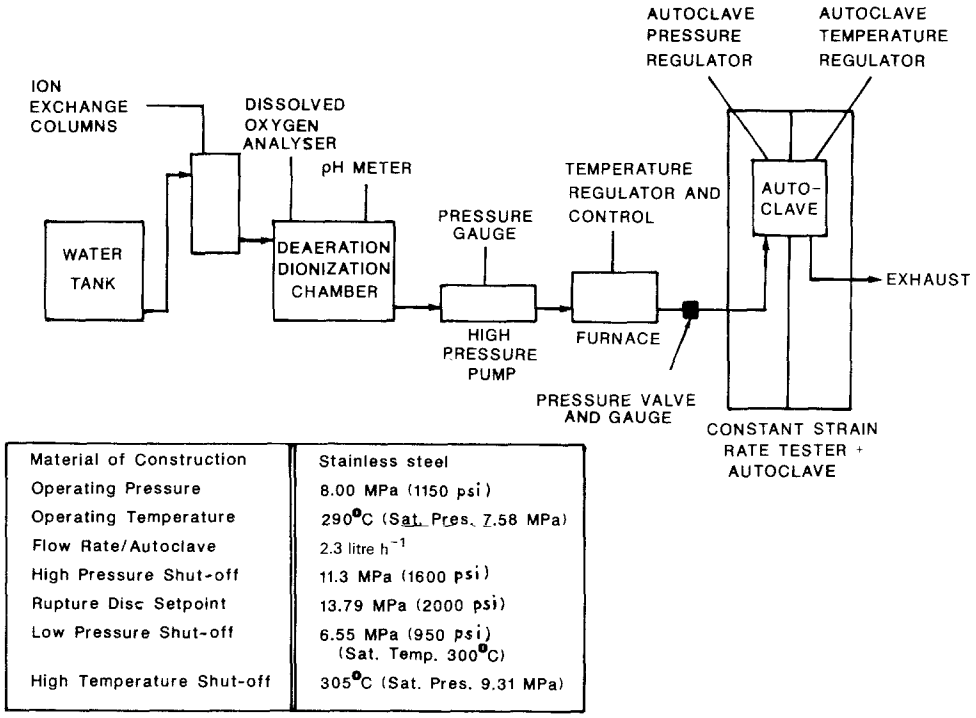

Figure 1 Schematic diagram and set-points of the autoclave system.

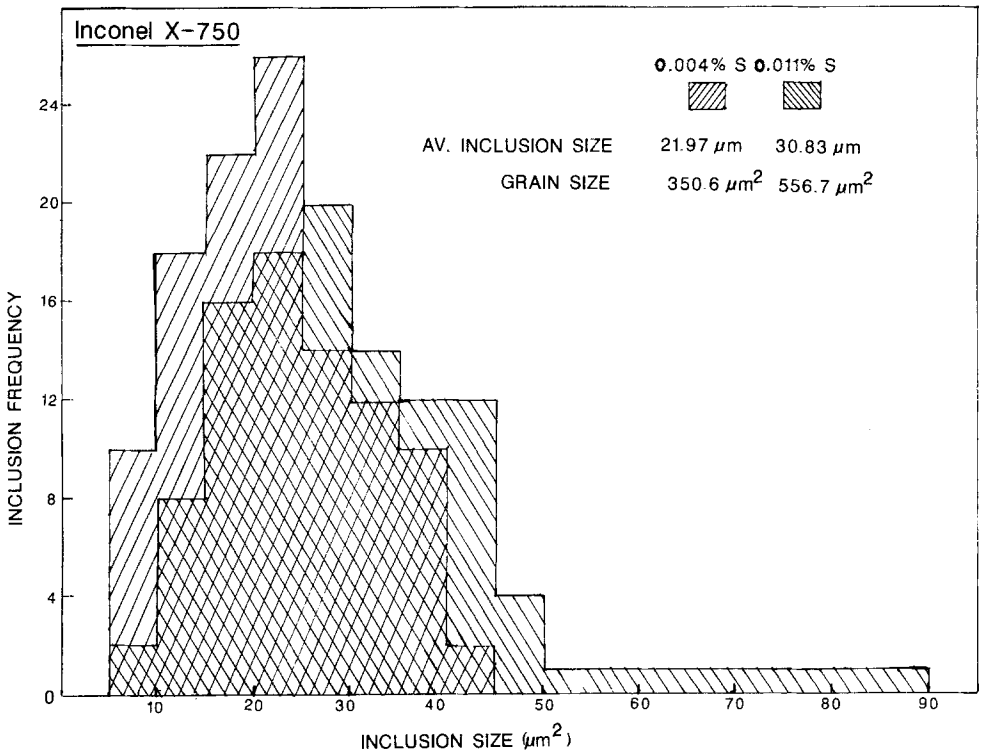

Figure 2 Inclusion distribution histogram of ESR and VAR alloys.

criterion was also supported by Charpy impact test results and modified Huey corrosion test results,[1].

Fig. 2 shows the inclusion distribution histogram of the ESR alloy containing 0.004% S and the VAR alloy containing 0.011% S. The average inclusion size for the ESR alloy was 21.97 μm, while, for the VAR alloy, it was 30.83 μm. The grain sizes for ESR- and VAR-treated alloys were 350 and 556.7 μm^2, respectively. The largest inclusion observed in the scanning area for the lower sulphur ESR material had a size of 45 μm while inclusions up to 90 μm size were seen for the VAR-processed alloy. The cleaner and grain-refined Inconel X-750 obtained by the ESR processing route produced a definite improvement in mechanical strength. The SSRT tests were performed using a superheated water medium having 5.9 pH and a dissolved oxygen level of 200 p.p.b.

Fig. 3 shows the load-displacement plots conducted in air at an initial strain rate of $2.8 \times 10^{-6} sec^{-1}$ for 0.011% S alloy for various ageing treatments. Similar curves were obtained for the 0.004% S alloy but the strengths were higher and the elongations lower than the high sulphur VAR-treated material for every ageing treatment. Tables II and III provide the mechanical property data for all the SSRT specimens in terms of per cent elongation, percent reduction in area, maximum and failure loads, and the time to failure for the two alloys.

The data on air and furnace cooled samples after 200 h ageing at 871° C shows that the lower sulphur material (ESR-treated) provided a relatively higher strength compared to the higher sulphur material, (VAR-treated). The furnace-cooled specimen exhibited a much improved tensile strength with a very small loss in toughness.

A comparison of the recorded data for specimens tested in air and PWR conditions showed a significant drop in strength in the smaller grain-size alloy while

TABLE II Slow strain rate test data for Inconel X-750 specimens. $\dot{\varepsilon} = 2.8 \times 10^{-6} sec^{-1}$, S = 0.004%

Specimen aged at	Elong. (%)	R.A. (%)	Maximum load (kN)	Load at failure (kN)	Time to failure (h)	Test medium
704° C, 2 h	37.4	46.0	34.9	31.8	37.4	Air
	38.7	46.0	29.1	26.7	38.7	PWR
704° C, 200 h	30.0	30.0	37.1	32.9	30.0	Air
	38.5	46.0	26.7	26.3	38.5	PWR
760° C, 100 h	31.4	32.0	36.7	32.5	31.4	Air
	31.0	32.0	28.8	26.6	31.0	PWR
871° C, 100 h	46.1	54.0	23.3	19.1	46.1	Air
	51.2	49.0	19.3	18.5	51.2	PWR
871° C, 200 h	44.0	50.0	25.3	19.4	44.0	Air
	53.4	50.0	20.6	18.2	53.4	PWR
871° C, 200 h (F)	33.5	38.0	32.8	29.8	33.5	Air
	34.0	40.0	29.9	26.2	34.0	PWR
As-quenched	52.9	51.7	15.3	19.6	52.9	Air
	67.8	60.2	20.1	17.4	67.8	PWR

F = furnace cooling from the ageing temperature.

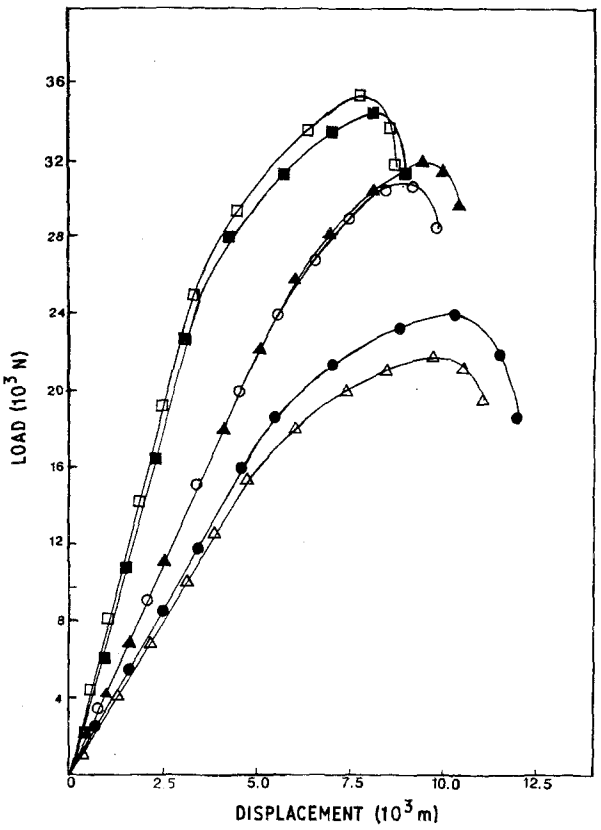

Figure 3 Load–displacement curves at a strain rate of $2.8 \times 10^{-6}\,sec^{-1}$ in air for Inconel X-750, 0.011% S. (●) 871° C, 200 h; (○) 871° C, 200 h (F); (■) 760° C, 100 h; (□) 704° C, 200 h; (▲) 704° C, 2 h; (△) 871° C 100 h. (F) indicates furnace cooling from the ageing temperature. All other specimens were air cooled from the ageing temperature.

the larger grained VAR treated specimens exhibited a relatively lower drop. The drop in strength when tested under PWR conditions. This is directly related to its susceptibility to stress corrosion cracking. A large drop in the total load (applied + pressure) and percentage elongation is indicative of a poor resistance to SCC, e.g. ageing at 704° C for 200 h for the 0.004% S alloy. Table IV gives the tensile data for the more conventional triple heat-treated condition, i.e. 1149° C/2 h, air cooled to 843° C/24 h, air cooled to 704° C/20 h and finally air cooled to room temperature, and shows a higher strength, when tested in air, compared with any single ageing treatment. However, the drop in strength, when tested under PWR conditions, is large and indicates poor resistance to SCC.

The stress corrosion cracking index, I_{SCC} [8], has been tabulated in Table V using the following relationship

$$I_{SCC} = \left[\left(\frac{1 + \varepsilon_m}{1 + \varepsilon_m^{SCC}}\right)\left(\frac{P_m}{P_m^{SCC}}\right)\right] - 1 \qquad (1)$$

where P_m and P_m^{SCC} are the maximum loads in air and in a corrosive medium, respectively; ε_m, ε_m^{SCC} are the strains at the maximum load in air and a corrosive medium, respectively. Therefore, a low I_{SCC} value indicates improved resistance to SCC.

Table V gives the I_{SCC} values at a strain rate of $2.8 \times 10^{-6}\,sec^{-1}$ for both the 0.011% and 0.004% S materials. The VAR-treated alloy containing 0.011% S, shows a lower I_{SCC} value compared with the ESR-treated X-750 alloy for various heat treatments. Fully aged specimens at 704° C for 200 h or 760° C for 100 h followed by air cooling have the highest susceptibility to stress corrosion cracking while ageing at 871° C for 200 h followed by furnace cooling provided the greatest resistance to SCC. The alloy X-750 in its triple heat-treated condition, having 0.004% S, and tested at a strain rate of $2.8 \times 10^{-6}\,sec^{-1}$ produced an I_{SCC} value of 0.587 which is indicative of a very poor resistance to SCC.

A 1240° C, 2 h solution anneal treatment was used to study the high-temperature annealing effect on the I_{SCC} index for the ESR processed alloy. This low sulphur alloy was tested after ageing treatments of 704° C for 200 h, air cooled; 760° C for 100 h, air cooled; and 871° C for 200 h, furnace cooled. This high-temperature anneal (compared with 1075° C) was used to increase the grain size of the ESR-treated alloy.

Fig. 4 shows photomicrographs of specimens solution treated at 1075, 1150 or 1240° C for 2 h followed by water quenching and further aged for 200 h at 704° C and cooled in air.

Increasing the solution temperature, however, also resulted in increased dissolution of precipitates (intermetallics and secondary carbides) in the fcc matrix. This is evident from the fact that the specimen solution treated at 1240° C for 2 h followed by water quenching did not possess any undissolved γ' particles (Fig. 4) and, therefore, the hardness value of this supersaturated solid solution was observed to be the lowest (R_D 19). Table VI lists the hardness values of

TABLE III Slow strain rate test data for Inconel X-750 specimens. $\dot{\varepsilon} = 2.8 \times 10^{-6}\,sec^{-1}$, S = 0.011%

Specimen aged at	Elong. (%)	R.A. (%)	Maximum load (kN)	Load at failure (kN)	Time to failure (h)	Test medium
704° C, 2 h	41.8	47.9	32.0	30.0	41.8	Air
	40.4	47.0	31.0	27.1	40.4	PWR
704° C, 200 h	34.5	40.0	34.9	31.0	34.5	Air
	28.0	30.0	30.8	29.2	28.0	PWR
760° C, 100 h	35.0	43.0	33.5	30.6	35.0	Air
	26.8	27.0	24.8	22.8	26.8	PWR
871° C, 200 h	47.0	52.0	24.2	18.6	47.0	Air
	43.7	47.6	23.2	20.9	43.7	PWR
871° C, 200 h (F)	36.5	45.0	30.2	28.1	36.5	Air
	31.6	32.0	28.1	26.4	31.6	PWR
As-quenched	57.4	55.0	14.8	11.3	57.4	Air
	70.0	60.2	16.5	15.0	70.0	PWR

F = furnace cooling from the ageing temperature.

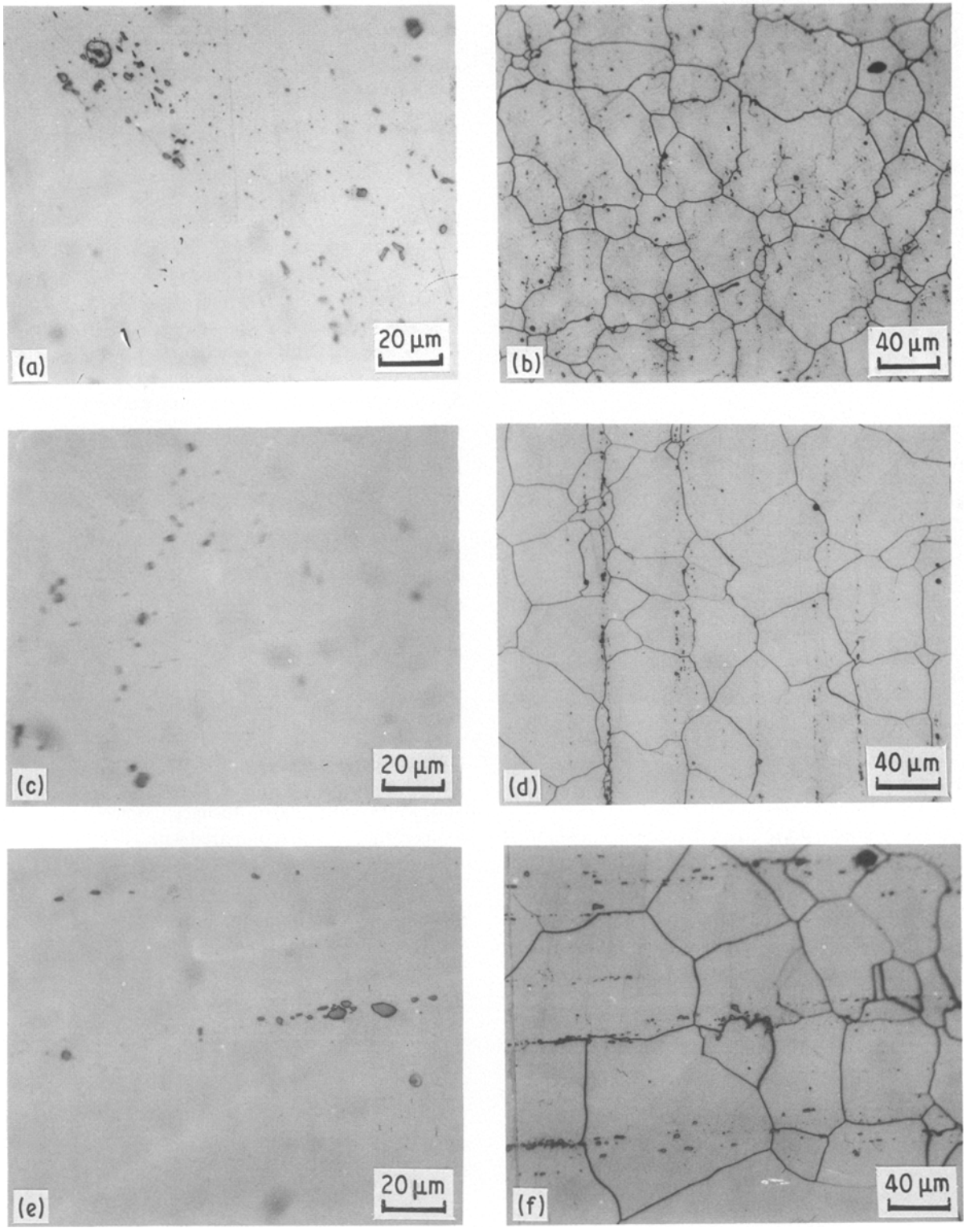

Figure 4 Photomicrographs of specimens treated at different solution temperatures, i.e. (a), (b) 1075° C; (c), (d) 1150° C; (e), (f) 1240° C each for 2 h. (a), (c) and (e) as-quenched; (b), (d) and (f) aged at 704° C for 200 h.

TABLE IV Slow strain rate test data for Inconel X-750 specimens. $\dot{\varepsilon} = 2.8 \times 10^{-6}\,\text{sec}^{-1}$, triple heat treatment

Specimen aged at	Elong. (%)	R.A. (%)	Maximum load (kN)	Load at failure (kN)	Time to failure (h)	Test medium
1149° C/2 h air cool to 843° C/2 h	27.7	29.6	39.3	35.9	27.7	Air
Air cool to 704° C/20 h, air cool	23.4	26.8	25.8	22.8	23.4	PWR condition

TABLE V Stress corrosion cracking index, I_{SCC}

Specimen aged at	I_{SCC}, Strain rate 2.8×10^{-6} sec^{-1}	
	0.004% S	0.011% S
704° C, 2 h	0.20	0.03
704° C, 200 h	0.37	0.24
760° C, 100 h	0.27	0.38
871° C, 100 h	0.20	0.11
871° C, 200 h	0.22	0.14
871° C, 200 h	0.10	0.08
Triple heat treatment	0.59	–

TABLE VI Hardness and grain size of over-aged specimens; 0.004% S

Solution treatment temperature (° C)	Hardness, R_D		Grain size (μm^2)
	As-quenched	704° C, 200 h ageing	
1075	25	54	372
1150	22	51	447
1240	19	49	508

these specimens and their grain sizes in the fully aged condition.

There was a 36% increase in the grain size for the specimen solutionized at 1240° C compared with that at 1075° C. Table VII lists the tensile properties for the 1240° C annealed specimens. Comparing these values with those in Table II and III, shows that there is a slight drop in the ultimate tensile strength. The stress corrosion cracking index listed in Table VIII for the 1240° C annealed specimens together with the data reproduced from Table V shows that there is an increase in the resistance to SCC when the solution treatment temperature is raised. For any of the ageing treatments used in the present study, a low-sulphur ESR alloy provided an enhancement in the SCC resistance when the solution treatment temperature was raised from 1075 to 1240° C. A more complete dissolution of precipitates and inclusions accompanied by grain growth at 1240° C is responsible for the loss in strength and gain in the SCC resistance.

An etch of 80 ml HNO_3 + 3 ml HF was used to attain and, therefore, emphasize the presence of secondary chromium carbides ($Cr_{23}C_6$) at the grain boundary rather than attacking the grain boundary itself. As is evident from Fig. 4, $Cr_{23}C_6$ is not precipitated at the grain boundary in the as-quenched condition.

Scanning electron microscopy together with the energy dispersive analysis using X-rays were performed on the fractured specimens from the SSRT tests to identify the failure mode, inclusion and precipitation sites and the response to a simulated PWR corrosive medium. A typical fractograph of one of the as-quenched specimens is shown in Fig. 5 where testing in the PWR medium shows evidence of primary carbide precipitation within the large dimples. This occurs while the specimen is held at 289° C for approximately 100 h during testing. There was no evidence of any such precipitation in the as-quenched specimen when tested in air. Figs 6a and b show the surface cracks which opened up during testing.

Fig. 7 compares the fracture morphology of a basically transgranular mode (871° C, 200 h furnace cooled) with a predominantly intergranular fracture mode (704° C, 200 h). Evidence of extensive micro-void coalescence is present in Figs 7c and d where a carbide-free grain-boundary area was observed under the optical microscope [1].

Segregation of FeS has been observed in the high-sulphur VAR alloy aged at 871° C for 200 h and air cooled. This alloy exhibited complete dissolution of secondary carbides at the grain boundary and the fractograph (Fig. 8) exhibited a fully transgranular ductile mode of fracture. Primary MC type carbides are still present within the grains (Fig. 8).

Fractographs of these SSRT specimens indicated that stress corrosion cracks appearing during the pressurized superheated water environment testing initiate at the inclusion or primary carbide sites and proceeded through the denuded zones (adjacent to the grain boundaries) because these phases are seen to be responsible for micro-void creation in the alloy.

4. Discussion

The use of the slow strain-rate technique as a method for detecting stress corrosion cracking susceptibility has an advantage over conventional testing techniques, such as static constant loading and U-bend, in that it promotes SCC in the system environment which, under static conditions, either do not crack or take a very long time to show any evidence of failure [9, 10]. This is a screening technique for detecting SCC susceptibility as it exposes specimens to the most prone condition for SCC failure. A range of 10^{-5} to 10^{-8} sec^{-1} strain rate has been known to cause SCC in most metallic systems [11].

The segregation effects are minimized in the ESR alloy as refining of molten metal is done in the form of slag-metal droplets. The effect of such refining

TABLE VII Slow strain rate test data for Inconel X-750 specimens. $\dot{\varepsilon}$ 2.8×10^{-6} sec^{-1}, S = 0.004%, annealing temperature 1240° C

Specimen aged at	Elong. (%)	R.A. (%)	Maximum load (kN)	Load at failure (kN)	Time to failure (h)	Test medium
704° C, 200 h	25.7	27.2	35.3	31.5	25.7	Air
	30.4	29.7	26.6	23.4	30.4	PWR
760° C, 100 h	26.4	28.1	34.4	31.0	26.4	Air
	27.8	29.2	26.3	23.3	27.8	PWR
871° C, 200 h (F)	32.3	30.0	30.7	28.6	32.3	Air
	35.3	40.7	28.1	26.9	35.3	PWR

F = furnace cooling from the ageing temperature.

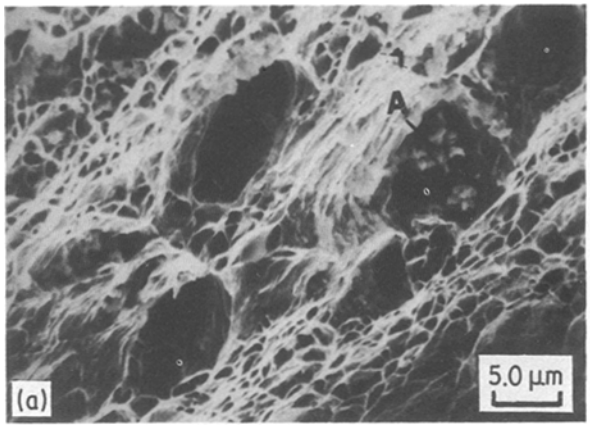

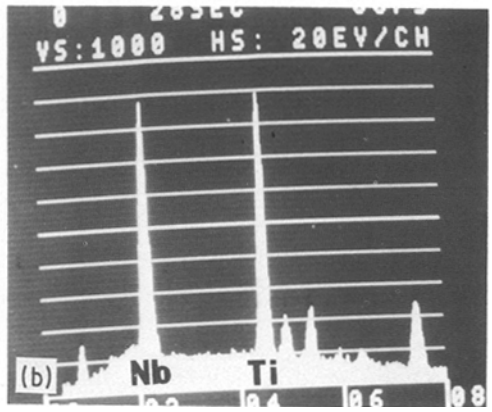

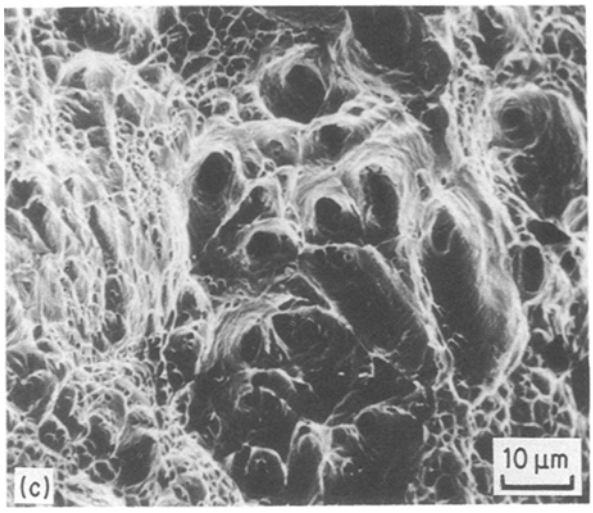

Figure 5 SEM fractographs of SSRT specimens for (a) as-quenched; tested under PWR conditions; (b) EDAX analysis at A in (a); (c) as-quenched, tested in air.

procedures on the mechanical and stress corrosion properties is largely governed by the size, shape and distribution of inclusions as well as the grain size.

The crevice produced by corrosion around sulphide inclusions can cause a local increase in stress intensity which may exceed K_{ISCC} and thus initiate cracking. If the applied stress is above the threshold, cracking will more readily initiate at the corrosion pits due to the stress concentration effect. Kiessling and Nordberg [12] have quantified the maximum defect size that the material can tolerate with the stress intensity factor not exceeding K_c values as $A = CK_I^2 (K_c)^2/\sigma_y$ where C has a value of 1.57 and 0.3 for a disc- and ellipsoid-shaped inclusion, respectively. K_I and σ_y are the safety factor and yield strength, respectively. It is possible to calculate the critical defect size from the K_{ISCC} data.

Sulphide inclusions may be directly responsible for producing the cracking species. It has been stated that both MnS and FeS seem to have sufficient solubility even in neutral water to give a significant concentration of HS^- ions, and to accelerate the corrosion reactions [13]. The tendency to crack may also increase due to absorbed hydrogen build up by the inhibition of the cathodic reaction: $2H^+ + 2e = H_2$, which sulphides are known to do. The inclusions often become detached during the early stages of corrosion and thus no obvious reason for the presence of a pit remains after further attack. It is the chemical activity of the inclusions which determines the extent to which they affect cracking and this is largely dependent upon their precise chemical composition, also their size and distribution. Sulphide inclusions are particularly active.

Sulphide inclusions from air melting are not significantly removed during VAR but there is a positive removal and uniform distribution during ESR. The VAR process also has a tendency to trap slag randomly

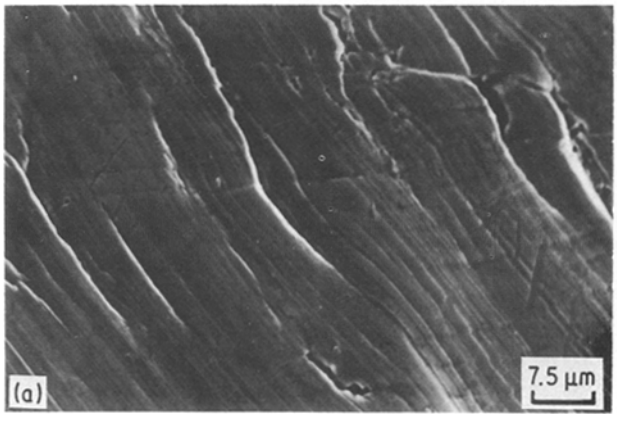

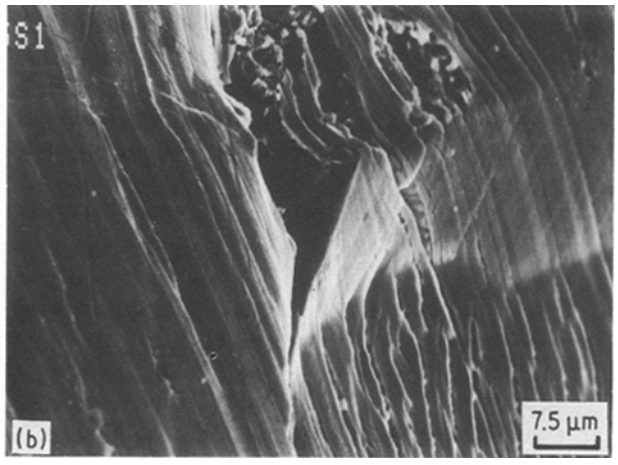

Figure 6 SEM fractographs showing surface deformation and cracks when aged at 704° C for 200 h; (a) tested in air, (b) tested under PWR conditions.

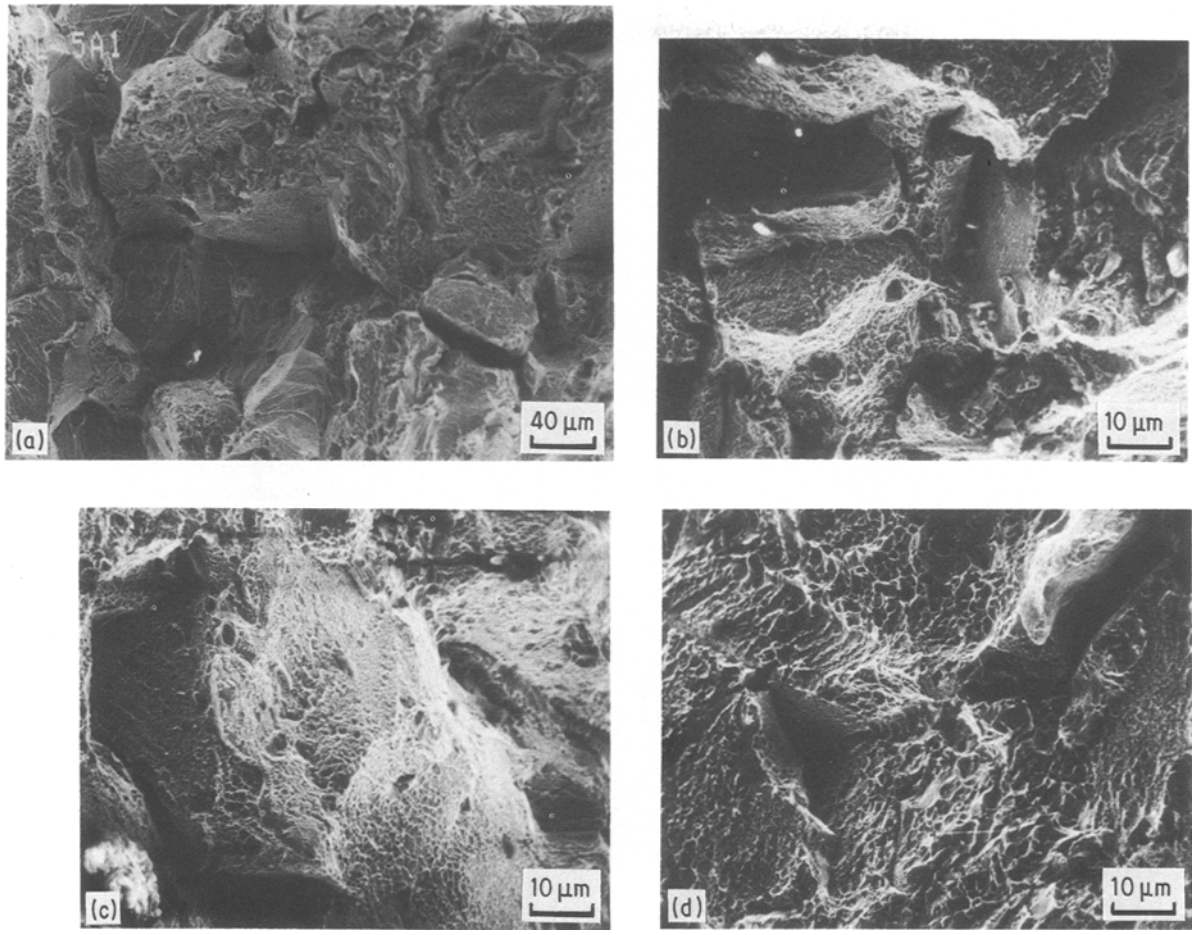

Figure 7 SEM fractographs of SSRT specimens (0.004% S) aged at: (a) 704° C for 200 h; tested in air, (b) 704° C for 200 h; tested under PWR conditions, (c) 871° C for 200 h; tested in air, (d) 871° C for 200 h; tested under PWR conditions.

which makes subsequent hot working useless [14]. These sulphide inclusions are detrimental to SCC because they are easily deformed in subsequent fabrication operations resulting in elongated stress raisers and regions of relatively easy crack propagation.

Testing in air at room temperature showed the highest strength for specimens aged at 704° C for 200 h and lowest for the as-quenched specimen. The PWR medium affected the fully aged specimens most, i.e. 704° C/200 h and 760° C/100 h, while its effect on the specimen aged at 871° C for 200 h followed by furnace cooling was the least. Anodic dissolution and/or hydrogen-assisted mechanisms are the modes of crack propagation which initiate at pits or at film rupture causing localized corrosion that forms corrosion trenches [15]. Therefore, the pH and oxygen level of the medium are critical for cracking under PWR conditions.

The results presented indicate that furnace cooling after 200 h ageing at 871° C provided the most resistance to stress corrosion cracking. In this condition, reprecipitation of secondary carbides and γ' at the grain boundary was observed along with primary carbide and phase precipitation in the intra-granular region [1]. The fully aged conditions of 704° C, 200 h and 760° C, 100 h, show a secondary carbide-depleted zone adjacent to the grain boundaries, which have fine γ' and primary MC carbide [16]. These are the prime stress concentration points and pit locations for crack initiation forming microvoids. These subsequently coalesce and propagate through the region exhibiting chromium depletion.

Ageing at 871° C for 100 to 200 h followed by air cooling exhibited a low susceptibility to I_{SCC} but was accompanied by a poor mechanical strength. Dissolution of carbides beyond 2 h ageing produced a zone entirely devoid of carbides at the grain boundaries. The failure mode was generally ductile in this case.

The restructuring of $M_{23}C_6$ type carbides at the grain boundary in the specimen aged at 871° C for 200 h and furnace cooled (Fig. 9) showed no significant depleted area as indicated by the Cr/Ni peak height ratios. Such a depleted region has been reported in the case of specimens aged at 704° C for 200 h and air cooled [16, 17]. Besides the strength achieved from this reprecipitation and phase formation from MC carbides, the absence of a depleted zone in the furnace cooled specimen aged at 871° C for 200 h significantly reduced the SCC susceptibility. A low I_{SCC} is indicative of this fact.

Comparison of the two sulphur level alloys in terms of I_{SCC} values and ultimate tensile strengths, it is observed that the ESR alloy (0.004% S; fine grain size) provides a higher strength while the VAR alloy (0.011% S; coarse grain size) provides a higher resistance to SCC. The finer grain size results in higher strength but a larger grain-boundary area for pronounced SCC effects. The coarse-grained VAR alloy

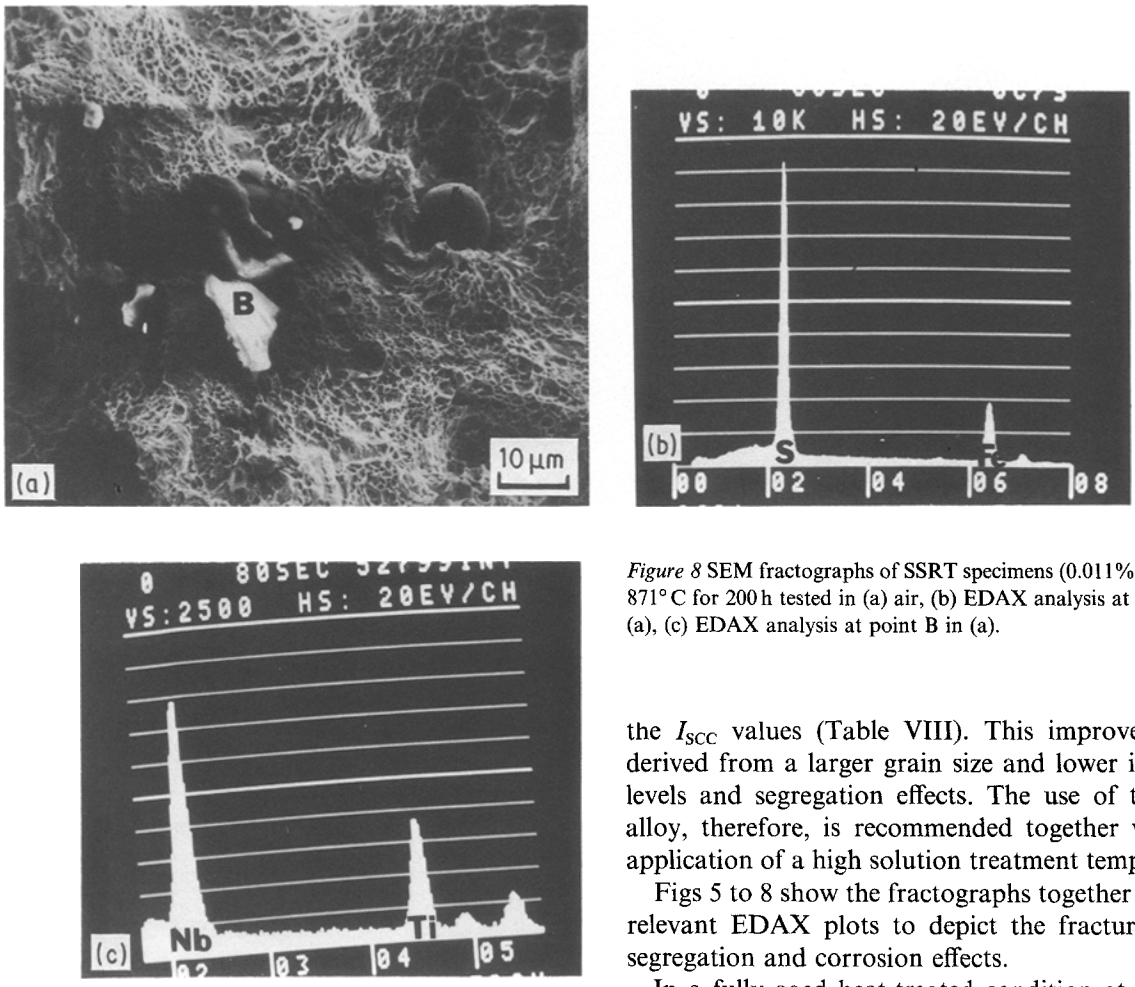

Figure 8 SEM fractographs of SSRT specimens (0.011% S) aged at 871° C for 200 h tested in (a) air, (b) EDAX analysis at point A in (a), (c) EDAX analysis at point B in (a).

results in a relatively lower strength but reduces IGSCC propagation. From the inclusion point of view, a cleaner alloy provides less crack nucleation sites. This observation holds good at any given heat treatment. Therefore, from the standpoint of improving IGSCC resistance, it was felt that a coarser grain size but cleaner alloy would be beneficial. A higher solutionizing temperature was, therefore, applied to the low sulphur ESR alloy.

Optical metallography performed on the ESR alloy specimen solution annealed at 1075, 1150 and 1240° C for 2 h and water quenched and further aged at 704° C for 200 h (Fig. 4) showed that there was virtually complete dissolution of all precipitates and inclusions at 1240° C, which was not achieved at 1075° C. The alloy strength was lower when compared with the 1075° C solutionized ESR processed specimens, but higher than the VAR alloys with the same heat treatment. There was a definite improvement in the I_{SCC} values (Table VIII). This improvement is derived from a larger grain size and lower inclusion levels and segregation effects. The use of the ESR alloy, therefore, is recommended together with the application of a high solution treatment temperature.

TABLE VIII Stress corrosion cracking index, I_{SCC}. $\dot{\varepsilon} = 2.8 \times 10^{-6}\,sec^{-1}$

Specimen aged at	I_{SCC}		
	0.004% S*	0.004% S†	0.011% S†
704° C, 200 h	0.28	0.37	0.27
760° C, 100 h	0.29	0.27	0.38
871° C, 200 h (F)	0.07	0.10	0.08

*1240° C anneal.
†1075° C anneal.

Figs 5 to 8 show the fractographs together with the relevant EDAX plots to depict the fracture mode, segregation and corrosion effects.

In a fully aged heat-treated condition at 704 and 760° C, the chromium-rich secondary carbide grain boundaries make the adjacent chromium-depleted areas very susceptible to cracking under stress corrosion conditions. Cracking is predominantly intergranular with the same transgranularity.

These fracture surfaces are associated with the breaking of intermediate and large cubic-shaped MC-type carbides, i.e. NbC, TiC, which eventually result in microvoids and quasi-cleavage fracture upon growth. A mechanism suggested for this behaviour is the movement of these facets ahead of the crack front, finally extending into the matrix by tearing causing microvoid coalescence [18]. A sufficiently high ductility and low flow stress produces these tearing regions, as observed adjacent to or between two large broken MC-type carbide containing dimples [18].

The surface cracks observed under PWR testing, however, did not change the primarily ductile mode of fracture for the specimen aged at 871° C for 200 h. Similar behaviour has been observed in austenitic stainless steel tested under high-temperature water conditions [11]. These surface cracks are mostly transgranular and dissolved inclusions act at sites for initiating these cracks when the electrochemical potential is favourable [19]. In A508 steels, the pits were formed due to the dissolution of MnS inclusions when the oxygen potential was high, i.e. 400 p.p.b. O_2. At lower oxygen levels crack initiation occurred circumferentially on the specimen surface without any localized corrosion [20].

Based on this work, it can be conclusively stated that Inconel X-750 alloy, solution annealed at 1240° C

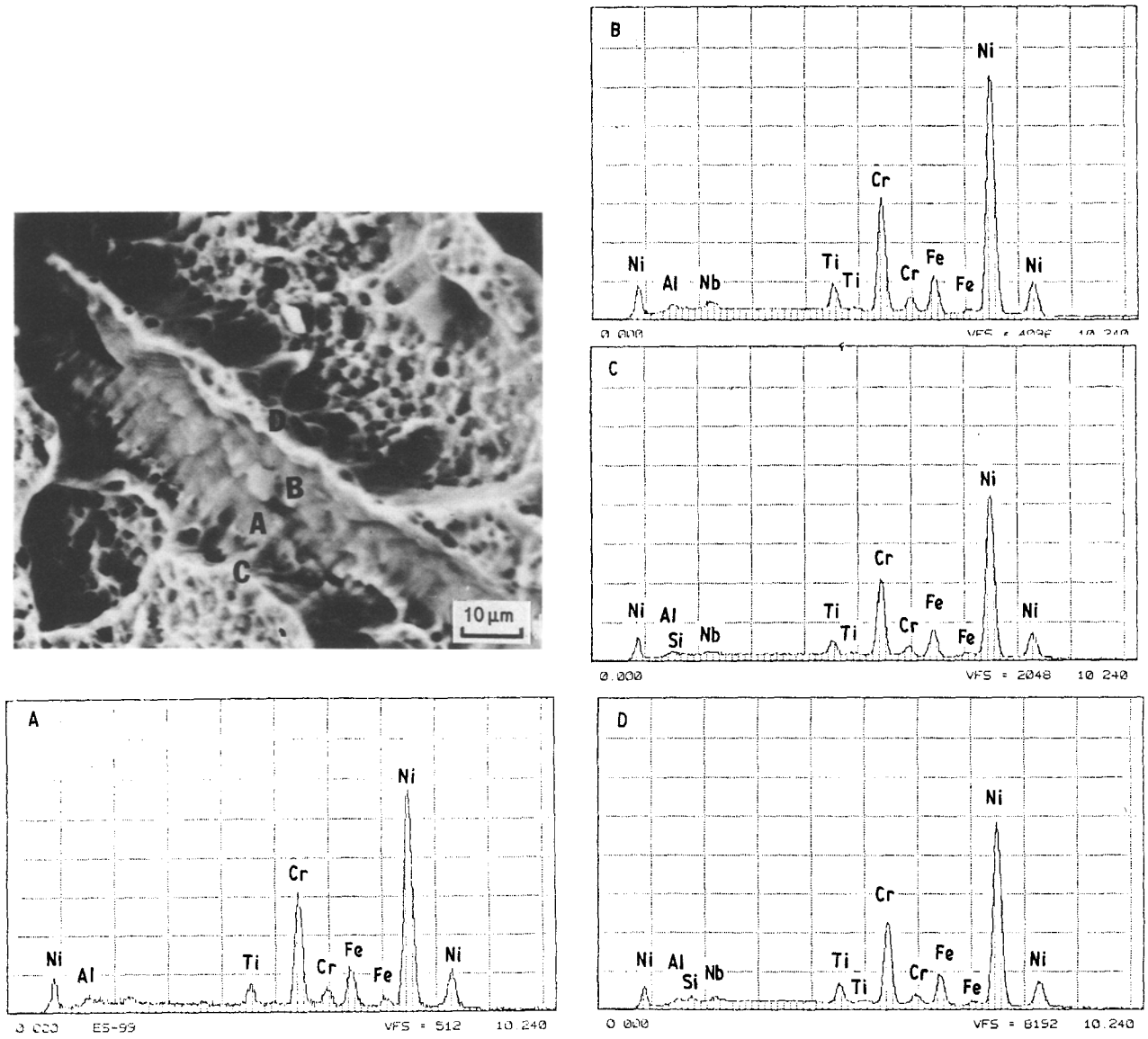

Figure 9 SEM fractographs and EDAX analysis of 871° C, 200 h aged and furnace-cooled specimen grain-boundary area.

for 2 h and water quenched, followed by ageing at 871° C for 200 h and furnace cooled, can be used to lower the susceptibility to IGSCC under PWR conditions. This processing route provides sufficient strength and ductility, a low I_{SCC} and a favourable fracture mode. The specimen surface, as well as the fractured surface, seems to indicate that an ESR-treated low-sulphur alloy should be preferentially used to lower the inclusion level, as these act as nucleation sites for crack initiation.

5. Conclusions

The stress corrosion cracking susceptibility of Inconel X-750 solution treated at 1075 and 1240° C for 2 h and aged between 704 and 871° C, observed in this work, allowed the following conclusions.

1. ESR alloy processing of Inconel X-750 produced a lower grain size, sulphur and inclusion level compared with VAR-processed material where sulphur was mostly present as FeS inclusions in the alloy.

2. Because of its larger grain size, the high-sulphur containing VAR-treated Inconel X-750 alloy was associated with a lower strength and a slightly higher ductility when tested at slow strain rates in air or the PWR medium.

3. The ESR-treated alloy had a relatively higher I_{SCC} than the VAR-treated steel for various heat treatments. Ageing at 704° C, 200 h or 760° C, 100 h exhibited poor resistance to IGSCC, in particular. The larger grain size of the VAR alloy was responsible for its lower I_{SCC}.

4. High-temperature austenitizing of the ESR alloy to increase the grain size and more completely dissolve the inclusions at 1240° C, had beneficial effects in terms of lowering the I_{SCC}.

5. Largely intergranular cracking coupled with some transgranularity were associated with specimens having a high I_{SCC}. Surface cracks were associated with testing in the PWR environment. A chromium-depleted zone adjacent to the secondary carbide-rich grain boundaries in the fully aged alloy gave rise to a higher susceptibility to stress corrosion cracking.

6. 871° C, 200 h ageing treatment after solution treatment at 1240° C for 2 h followed by furnace cooling produced the best combination of strength, ductility and IGSCC resistance.

Acknowledgements

The authors thank the University of Minnesota for Doctoral Dissertation Fellowship and Dow Chemicals for a Special Dissertation Grant. They also thank CorTest, Inc., Willoughby, Ohio, for their financial support.

References

1. B. MISHRA, J. J. MOORE and A. K. SINHA, *Met. Trans.* **16A** (1985) 821.
2. S. HATTORI, Y. MORI, L. MASAOKA, H. ITCH and R. WATANABE, Hitachi Research Laboratory, Hitachi Ltd, Japan.
3. L. TRANSTAD and J. SEJERSTED, *J.I.S.I.* **127** (1933) 425.
4. G. EKLUND, *Jernkont Ann.* **155** (1971) 637.
5. *Idem, J. Electrochem. Soc.* **121** (1974) 467.
6. *Idem, Scand. J. Met.* **1** (1972) 331.
7. T. R. MAGER and R. S. ASPDEN, "Effects of Thermal History and Microstructure on the SCC Behaviour of Inconel X-750 in Aqueous Systems at 343 to 360° C", Westinghouse Research and Development Centre, Pittsburg, Pennsylvania, June 1976.
8. M. HISHIDA and H. NAKADA, *Corrosion* **33** (Bo. 11) (1977) 403.
9. "Stress Corrosion Cracking: The Slow-strain Rate Technique" ASTM-STP 665 (American Society for Testing and Materials, Philadelphia Pennsylvania, 1971).
10. R. N. PARKINS, in "Development of Strain Rate Testing and its Implication", ASTM STP 665, (American Society for Testing and Materials. Philadelphia, Pennsylvania, 1971) p. 5.
11. H. D. SOLOMON, M. J. POVICH and T. M. DEVINE, in "Slow Strain-rate Testing in High Temperature Water", ASTM-STP 665, (American Society for Testing and Materials, Philadelphia, Pennsylvania 1971) p. 132.
12. R. KIESSLING and H. NORDBERG, Proceedings International Symposium on "Production and Application of Clean Steels", Botonfured, Hungary (1972).
13. J. G. PARKER, Proceedings International Symposium on "Sulfide Inclusion in Steels" (ASM, Ohio, 1976) p. 403.
14. K. C. BARRACLOUGH, *Iron Making and Steel Making* **3** (1974) 172.
15. J. E. TRUMAN, *Corros. Sci.* **17** (1977) 737.
16. A. K. SINHA, PhD Thesis, University of Minnesota (1984).
17. L. E. HALL and C. L. BRIANT, *Met. Trans.* **16A** (1985) 1225.
18. B. MISHRA, J. J. MOORE, A. K. SINHA and M. G. HEBSUR, "Heat Treatment Effect on Mechanical Properties and Microstructure of Inconel X-750", 113th Annual AIME Meeting, Los Angeles, California, February 1984.
19. H. CHOI, F. H. BECK, Z. SZKLARSKA-SMIALOWSKA and D. D. MacDONALD, *Corrosion* **38** (1982) 136.
20. K. KLEMETTI and H. HANNINEN, Metals Laboratory, SF-02150, Espoo, Finland (1985).

Received 11 August 1986
and accepted 17 August 1987